RAA 2016 Vol. **16** No. **10**, 160 (6pp) doi: 10.1088/1674–4527/16/10/160
http://www.raa-journal.org *http://iopscience.iop.org/raa*

***R**esearch in*
***A**stronomy and*
***A**strophysics*

Accreting He-rich material onto carbon-oxygen white dwarfs until explosive carbon ignition

Cheng-Yuan Wu[1,2,3], Dong-Dong Liu[1,2,3], Wei-Hong Zhou[2,4] and Bo Wang[1,2]

[1] Yunnan Observatories, Chinese Academy of Sciences, Kunming 650216, China; *wcy@ynao.ac.cn; wangbo@ynao.ac.cn*
[2] Key Laboratory for the Structure and Evolution of Celestial Objects, Chinese Academy of Sciences, Kunming 650216, China
[3] University of Chinese Academy of Sciences, Beijing 100049, China
[4] Yunnan Minzu University, Kunming 650031, China

Received 2016 February 5; accepted 2016 June 30

Abstract Type Ia supernovae (SNe Ia) play an important role in studies of cosmology and galactic chemical evolution. They are believed to be thermonuclear explosions of carbon-oxygen white dwarfs (CO WDs) when their masses approach the Chandrasekar (Ch) mass limit. However, it is still not completely understood how a CO WD increases its mass to the Ch-mass limit in the classical single-degenerate (SD) model. In this paper, we studied the mass accretion process in the SD model to examine whether the WD can explode as an SN Ia. Employing the stellar evolution code called modules for experiments in stellar astrophysics (MESA), we simulated the He accretion process onto CO WDs. We found that the WD can increase its mass to the Ch-mass limit through the SD model and explosive carbon ignition finally occurs in its center, which will lead to an SN Ia explosion. Our results imply that SNe Ia can be produced from the SD model through steady helium accretion. Moreover, this work can provide initial input parameters for explosion models of SNe Ia.

Key words: stars: evolution — binaries: close — supernovae: general — white dwarfs

1 INTRODUCTION

Type Ia supernova (SN Ia) explosions are among the most energetic phenomena in the Universe. They have successfully been used as standard cosmological distance indicators due to their uniformly high luminosities. SNe Ia acting as standard candles have revealed the acceleration of the expansion of the Universe, which indicates the existence of dark energy (e.g., Riess et al. 1998; Perlmutter et al. 1999). SN Ia explosions also play an important role in producing heavy chemical elements (e.g., Greggio & Renzini 1983; Matteucci & Greggio 1986). Moreover, they are accelerators of cosmic rays (e.g., Fang & Zhang 2012; Yang et al. 2015). However, the progenitors of SNe Ia and their explosion mechanisms are still unclear, which may directly influence the accuracy of cosmological results inferred from SN Ia distances and current models of galactic chemical evolution (e.g., Podsiadlowski et al. 2008; Howell 2011; Wang & Han 2012; Maoz et al. 2014).[1]

It is widely believed that SNe Ia arise from thermonuclear runaway explosions of carbon-oxygen white dwarfs (CO WDs) in binaries (e.g., Hoyle & Fowler 1960; Nomoto et al. 1997). When a CO WD increases its mass to the Chandrasekar (Ch) mass limit, the carbon in its center will be ignited. Then, the whole WD will be destroyed by explosive carbon burning in the degenerate core. Up to now, there have been several explosion models proposed for SNe Ia, such as the carbon detonation supernova model (e.g., Arnett 1969), the carbon deflagration model (e.g., Nomoto et al. 1976; Nomoto et al. 1984), the delayed detonation model (e.g., Khokhlov 1991), and the double detonation model (e.g., Taam 1980; Nomoto 1982a; Livne 1990). At present, there are two popular progenitor models for SNe Ia, which are the single-degenerate (SD) model and the double-degenerate (DD) model. For the SD model, a WD accretes H- or He-rich material from its non-degenerate companion and increases its mass to approach the Ch-mass limit. The non-degenerate companion could be a main sequence star, a red giant star, an He star or even an asymptotic giant branch star (e.g., Whelan & Iben 1973; Nomoto et al. 1984; Hachisu et al. 1996; Li & van den Heuvel 1997; Langer et al. 2000; Hamuy et al. 2003;

[1] SNe Ia are the main contributors of iron to their host galaxies, and the iron galactic distribution generally depends on SN Ia evolutionary timescales. Thus, identification of the progenitors of SNe Ia is crucially important for galactic chemical evolution (e.g., Matteucci & Greggio 1986).

Han & Podsiadlowski 2004; Wang et al. 2009a, 2014). For the DD model, SNe Ia originate from the merging of two CO WDs in the Hubble time, which have a combined mass larger than the Ch-mass limit. In this model, both of the WDs are brought together due to the loss of orbital angular momentum, which is driven by gravitational wave radiation (e.g., Webbink 1984; Iben & Tutukov 1984).

The SD model has been supported by some evidence in observations. Tycho G is thought to be the surviving companion of Tycho's SN (e.g., Ruiz-Lapuente et al. 2004), and its parameters (e.g., space velocity, surface gravity and effective temperature) are compatible with the properties of surviving companions from the SD model (e.g., Han 2008; Wang & Han 2010a). Some direct evidence of circumstellar material has been found in some SNe Ia, which supports the SD model (e.g., Patat et al. 2007a,b; Wang et al. 2009b). Moreover, the presence of a non-degenerate companion in the SD model could leave an observable trace in the form of ultraviolet (UV) emission, and the interaction between SN ejecta and its companion can be detected in UV emission, which may indicate the presence of a non-degenerate donor in their progenitor systems (e.g., Kasen 2010; Hayden et al. 2010). Moreover, in observations a number of WD binaries, e.g., U Sco (a WD + main sequence system), RS Oph (a WD + red giant system), TCrB (a WD + red giant system), V445 Pup (a WD + He star system) and HD 49798 with its WD companion (a WD + He star system), have been identified as possible candidates for SD progenitors of SNe Ia (e.g., Israel et al. 1997; Parthasarathy et al. 2007; Woudt et al. 2009; Wang & Han 2010b).

In the SD model, most of the previous works have treated WDs as point masses instead of solving stellar structure equations of WDs when calculating the mass-transfer process. Accreted material is burned into carbon and oxygen on the surface of a WD, and the WD has been thought to explode as an SN Ia once its mass grows to the Ch-mass limit, (e.g., Hachisu et al. 1996, 1999; Chen & Li 2009; Wang et al. 2010; Ablimit et al. 2014). In this work, we will simulate the He accretion onto CO WDs by considering the structure of WDs until the explosive carbon ignition occurs in the center of WDs.

This article is organized as follows. The basic assumptions and methods for numerical calculations are given in Section 2. In Section 3, we present the results of our calculations. Finally, the discussion and conclusions are provided in Section 4.

2 METHODS

We employ the stellar evolution code called Modules for Experiments in Stellar Astrophysics (MESA) to simulate the mass accretion process of He-rich material onto CO WDs (see Paxton et al. 2011, 2013, 2015). MESA is an efficient application in computational stellar astrophysics. This code is powerful for studying progenitors of SNe Ia (e.g., Ma et al. 2013; Chen et al. 2014, 2015; Wang et al. 2015; Brooks et al. 2016). In particular, we note that Denissenkov (2012); Denissenkov et al. (2013) have successfully used MESA to simulate the process of nova outbursts. Here, we adopt two suite cases (`make_co_wd` and `wd2`) in MESA to perform our simulations. The suite case `make_co_wd` is used to create initial models of CO WDs, whereas the suite case `wd2` is used to simulate the accretion process onto WDs. We use the default OPAL opacity in our simulations (see Iglesias & Rogers 1996), and the nuclear reaction network `co_burn.net` is adopted. This nuclear reaction network consists of isotopes needed for hydrogen, helium, carbon and oxygen burning (i.e., ^{1}H, ^{3}He, ^{4}He, ^{12}C, ^{14}N, ^{16}O, ^{20}Ne, ^{24}Mg, ^{28}Si), which coupled by 57 reactions. In addition, we have considered the carbon burning $^{12}\mathrm{C}+{}^{12}\mathrm{C}$ nuclear fusion in dense matter (see Gasques et al. 2005). This has some influence on the $^{12}\mathrm{C}+{}^{12}\mathrm{C}$ nuclear reaction rate which is not included in the nuclear reaction network `co_burn.net`.

First, we use the suite case `make_co_wd` to construct CO WD models (see also Denissenkov et al. 2013). We create a sufficiently massive pre-main sequence model with H mass fraction $X = 0.7$ and metallicity $Z = 0.02$, and evolve it through the main sequence stage and the red giant branch. We remove the outer envelope of the star artificially once it reaches the asymptotic giant branch, leaving a pure CO core. After that, the star becomes a CO WD and arrives at the WD cooling phase.

Second, the suite case `wd2` is used to calculate the process of mass accretion onto the surface of WDs. Using the WD model that we constructed and the suite case `wd2`, we simulate the steady He accretion process onto a WD with an initial mass of $0.8\,M_{\odot}$. The initial central temperature ($T_{\rm c}$) and density ($\rho_{\rm c}$) of the WD are 6.9×10^{7} K and $7.0\times10^{7}\,{\rm g\,cm^{-3}}$, respectively. The WD accretes He-rich material at the rate of $1.6\times10^{-6}\,M_{\odot}\,{\rm yr^{-1}}$, which is an accretion rate in the steady burning regime of a $0.8\,M_{\odot}$ WD (see Piersanti et al. 2014; Wang et al. 2015). If the accretion rate is higher than $2\times10^{-6}\,M_{\odot}\,{\rm yr^{-1}}$, the WD will become a red giant-like star (e.g., Nomoto 1982b). If the accretion rate is lower than $1\times10^{-6}\,M_{\odot}\,{\rm yr^{-1}}$, the accumulated He-rich material is degenerate, and nova outbursts happen (e.g., Kato & Hachisu 2004). If the accretion rate is too low (e.g., lower than $4\times10^{-8}\,M_{\odot}\,{\rm yr^{-1}}$), then He detonation may be triggered (e.g., Nomoto 1982a). The He mass fraction and metallicity of accreted material were set to be 0.98 and 0.02, respectively. In our simulation, we compute over 20 000 models and resolve the WD into more than 2000 mass shells. After long-term evolution, we obtained explosive carbon ignition in the center of the CO WD at the end of our calculations.

When the CO WD evolves to the explosive carbon ignition, a huge amount of energy has been released by carbon burning, and thermal runaway finally happens, resulting in an SN Ia. However, there are still a lot of uncertain factors about when explosive carbon ignition happens. Lesaffre et al. (2006) assumed that an SN Ia can be produced once the CO WD evolves to the point $t_{\rm b}=\frac{1}{22}t_{\rm c}$. Here $t_{\rm b}$ is the differential burning timescale ($t_{\rm b}^{-1}=\frac{q}{c_{\rm p}T}$),

and $t_{\rm c}$ is a convective element's crossing time over a pressure scaleheight ($t_{\rm c} = \frac{H_{\rm p}}{u_{\rm c}}$), in which T is the temperature, $c_{\rm p}$ is the specific heat at constant pressure, q is the rate of energy generation due to carbon burning, $H_{\rm p}$ is the pressure scaleheight, and $u_{\rm c}$ is the convective velocity as given by mixing length theory. Note that the adopted explosive carbon ignition criterion $t_{\rm b} = \frac{1}{22}t_{\rm c}$ may differ in different works and lead to uncertainties (e.g., Lesaffre et al. 2006). In order to remove this uncertainty, we continue our calculations after the CO WD passes through the point in which $t_{\rm b} = \frac{1}{22}t_{\rm c}$, and found that the temperature in the center finally increases sharply but the density does not change any more. In our simulations, we adopt the starting point of the central temperature dramatically increasing as the explosive carbon ignition point (see also Chen et al. 2014).[2]

3 RESULTS

Figure 1 shows the evolution of the luminosity, radius and mass of the CO WD changing with time during the steady He burning stage, in which the initial mass of the WD is $0.8\,M_\odot$ and the accretion rate is $1.6\times10^{-6}\,M_\odot\,{\rm yr}^{-1}$. The He-shell burning transforms the He-rich material into carbon and oxygen which, as a result, accumulates mass in the CO core. The WD can increase its mass steadily until it grows to $1.386\,M_\odot$, which lasts for about 3.6×10^5 years. At the beginning of the He accretion, the radius and luminosity increase with the accumulation of the accreted He-rich material on the surface of the WD. When the nuclear burning rate at the bottom of the He-shell goes up, the burning rate of the He-rich material almost equals the accretion rate, which prevents the mass of the He shell from increasing. In this case, the radius and luminosity decrease due to the shrinking of the CO core.

Figure 2 presents the Hertzsprung-Russell (HR) diagram of the accreting CO WD. At the onset of accretion, the luminosity of the WD increases but the effective temperature decreases due to the extension of the radius. The effective temperature increases steadily once the WD begins to shrink. When the mass of the WD is larger than $1.1\,M_\odot$, the accretion rate $1.6\times10^6\,M_\odot\,{\rm yr}^{-1}$ is near the bottom of the steady burning regime (the top of the He-flash regime) (see Piersanti et al. 2014). Then, the He burning becomes a slight instability and forms the fluctuating features in the HR diagram. At the final stage of the accretion process, the WD grows close to $1.386\,M_\odot$, and the nuclear reaction rate in its center increases sharply but the luminosity drops rapidly. This process takes 45 years until explosive carbon ignition occurs.

In Figure 3, we show the central density and temperature of the WD during the mass accretion. The density and temperature in the center of the WD increase with the WD mass when it accretes He-rich material steadily. At the end of the mass accretion, the nuclear reaction rate in the center of the WD increases rapidly but the density does not change any more. We note that the criterion of explosive carbon ignition adopted in Lesaffre et al. (2006) is the point where $t_{\rm b} = \frac{1}{22}t_{\rm c}$ (the green mark in Fig. 3). The criterion used in our simulation is the point where central temperature starts increasing dramatically, which is closer to the explosion (the red mark in Fig. 3).

Figure 4 shows the density-temperature profile of the CO WD at the moment of explosive carbon ignition (see the red filled dot in Fig. 3). There are three burning regions in the WD, i.e., He layer burning, surface carbon burning and central carbon burning. Among these, the total energy is determined by the central carbon burning, in which the nuclear reaction rate at the moment of the explosive carbon ignition has risen to $10^{15}\,{\rm erg\,g^{-1}\,s^{-1}}$. Meanwhile, $T_{\rm c}$ and $\rho_{\rm c}$ grow to 1.1×10^9 K and $2.44\times10^9\,{\rm g\,cm^{-3}}$, respectively. At this moment, the convective velocity of the carbon burning regime is 0.022 times the local sound speed and the convection region has developed from the center to the position where the mass coordinate is $0.805\,M_{\rm WD}$.

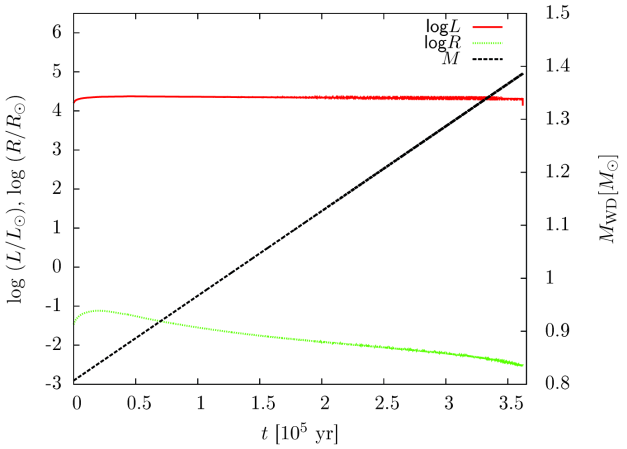

Fig. 1 Long-term evolution of a $0.8\,M_\odot$ accreting WD until its mass increases to the Ch-mass limit. The evolution of the luminosity, radius and mass as a function of time are shown in this figure, in which $\dot{M}_{\rm acc} = 1.6\times10^{-6}\,M_\odot\,{\rm yr}^{-1}$.

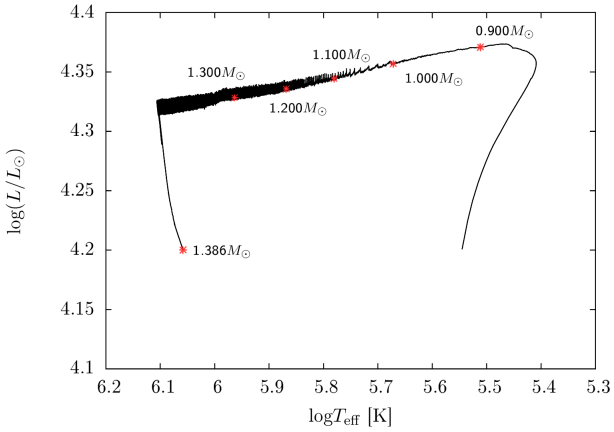

Fig. 2 Long-term evolution of the $0.8\,M_\odot$ CO WD during mass accretion in the HR diagram. Red marks indicate the WD mass at given points.

[2] Chen et al. (2014) recently studied the process of accreting CO-rich material onto CO WDs until explosive carbon ignition.

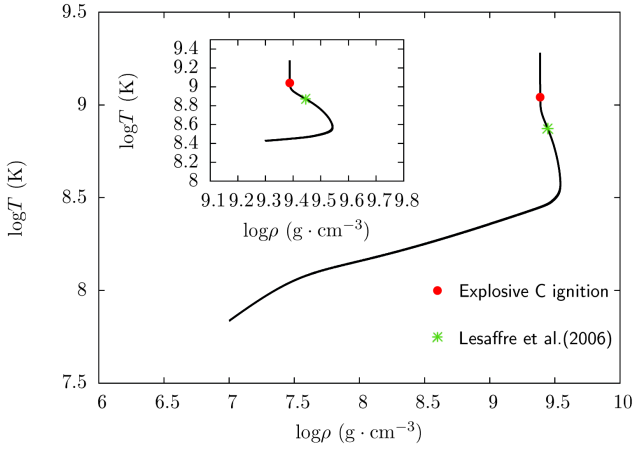

Fig. 3 Central density and temperature profile for the evolution of the $0.8\,M_{\odot}$ CO WD during mass accretion. The inset panel shows the final phase of the entire evolution. The green mark shows the point of explosive carbon ignition where $t_{\rm b} = \frac{1}{22}t_{\rm c}$ (see Lesaffre et al. 2006), whereas the red mark represents the point of explosive carbon ignition that we adopted.

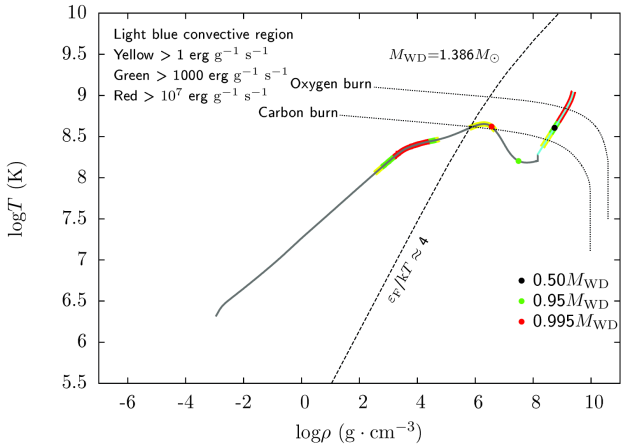

Fig. 4 Density and temperature profile at the moment of explosive carbon ignition. $M_{\rm WD}$ is the WD mass at the moment of explosive carbon ignition. The dotted lines are the conditions for carbon and oxygen nuclear reactions. The dashed line shows the separation of degenerate and non-degenerate regions ($\varepsilon_{\rm F}/kT \approx 4$). Light blue indicates the convective region, while grey signifies the non-convective region. Yellow, green and red show the energy production rates of nuclear reactions. Red, green and black dots represent the different mass fraction points inside the WD.

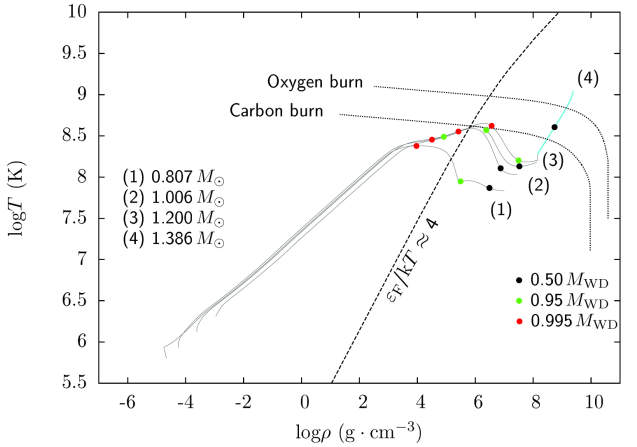

Fig. 5 Similar to Figure 4, but for various phases during mass accretion. Numbers (1)−(4) indicate the different phases from initial accretion to final explosive carbon ignition, and the WD mass for each number is indicated in this figure.

Also at this moment, the deflagration is transforming from inside out in the form of subsonic flame propagation.

In Figure 5, we show the density-temperature profile of the WD at various phases during mass accretion. At the onset of accretion, the accreted material is compressed and releases gravothermal energy on the surface of the CO WD. The thermal energy can hardly diffuse into the inward region because the WD is highly compressed. Thus, all of the released gravothermal energy is stored as thermal energy, leading the surface temperature to increase sharply but the interior changes little. With the increase of the surface temperature, the released energy begins to transfer into underlying zones. After that, the surface changes slowly, and central temperature and density increase rapidly. Eventually, the central temperature is high enough for carbon ignition, and convection has developed in the center of the WD until explosive carbon ignition.

4 DISCUSSION AND CONCLUSIONS

In this work, we only studied the He accretion onto WDs, and the WD can increase its mass to the Ch-mass limit. In the SD model, a CO WD can also accrete H-rich material from its companion, and then explode as an SN Ia. The accumulated H-rich material on their surface can be burned into He and then transformed into carbon and oxygen, resulting in the mass increase of WDs. However in previous studies, it was difficult to increase the WD mass to the Ch-mass limit by considering the double-shell (H and He) burning process (e.g., Hillman et al. 2016). Further theoretical studies of double-shell burning are needed.

In addition, we did not consider the influence of rotation on the mass accretion. Yoon et al. (2004) have found that He burning becomes less violent on the surface of a WD when considering rotation, and the He accretion efficiency may be higher than the condition of non-rotation. Moreover, rotation may increase the upper stable mass limit of the WD, and may produce a WD whose mass is above the Ch-mass limit (e.g., Yoon & Langer 2005).

Previous works found that the accretion rate plays a crucial role in the evolution of accreting WDs. If the accretion rate is too low, accreting WDs may undergo multicycle He-shell flashes like nova outbursts (e.g., Kato & Hachisu 2004). If the accretion rate is too high, the WD will become a red giant-like He star (e.g., Nomoto 1982b). Thus, the He-shell can only be burned into carbon and oxygen steadily in a narrow regime. We also note that if the accretion rate is lower than $4 \times 10^{-8}\,M_{\odot}\,\mathrm{yr}^{-1}$, the He flash on the surface of the WD is so strong that an He detonation wave propagates outward, while an inward propagating pressure wave compresses the CO core that triggers an outward detonation, leading to an SN Ia explosion based on the double detonation model (e.g., Woosley & Weaver 1986; Piersanti et al. 2014). In this work, we only focus on the steady burning regime and the He can be completely transformed into carbon and oxygen at the accretion rate, in which the WD can increase its mass to the Ch-mass limit.

It is widely known that the carbon reaction rate is important for thermonuclear explosions of CO WDs. For the ranges of $T \sim (1.5-7)\times10^{8}$ K and $\rho \sim (2-5)\times10^{9}\,\mathrm{g\,cm^{-3}}$, the timescale and ignition conditions are determined by the $^{12}\mathrm{C}+{}^{12}\mathrm{C}$ reaction rate (e.g., Woosley et al. 2004; Baraffe et al. 2004). Under the high temperature and density in the centers of WDs, carbon is fully ionized. The $^{12}\mathrm{C}$ reaction rate is more sensitive to changes in T than ρ, and the repulsive Coulomb barrier between interacting $^{12}\mathrm{C}$ nuclei can be reduced by the influence of strong plasma screening (see Gasques et al. 2005). Thus, we adopted the $^{12}\mathrm{C}+{}^{12}\mathrm{C}$ revised reaction in dense material in this work. We also simulated the He accretion process by ignoring the $^{12}\mathrm{C}+{}^{12}\mathrm{C}$ revised reaction rate, and found that the WD has higher central temperature but lower central density at the moment of explosive carbon ignition.

By employing the stellar evolution code MESA, we have investigated the long-term evolution of an He-accreting CO WD. We found that He-rich material can be burned steadily on the surface of a $0.8\,M_{\odot}$ WD with an accretion rate of $1.6\times10^{-6}\,M_{\odot}\,\mathrm{yr}^{-1}$. Eventually, explosive carbon ignition happens in the center of the CO WD when it increases its mass to the Ch-mass limit. Our results can provide initial input parameters for explosion models of SNe Ia. Importantly, our results indicate that SNe Ia can be produced through the SD model. We note that a massive CO WD may lead to a lower ratio of carbon to oxygen, and thus the less amount of $^{56}\mathrm{Ni}$ synthesized in the thermonuclear explosion can produce a lower luminosity of SNe Ia (e.g., Arnett 1982). Moreover, luminous SNe Ia preferably occur in relatively metal poor environments (e.g., Neill et al. 2009; Taubenberger et al. 2011). In future studies, we will calculate the He accretion onto WDs with different initial masses, accretion rates and metallicities to examine their influence on the final results.

Acknowledgements We acknowledge useful comments and suggestions from the referee. We thank Zhanwen Han, Yan Li and Xuefei Chen for their helpful discussions. This work is supported by the National Basic Research Program of China (973 program, 2014CB845700), the National Natural Science Foundation of China (Nos. 11322327, 11390374, 11521303 and 61561053), the Chinese Academy of Sciences (Nos. KJZD-EW-M06-01 and XDB09010202), the Natural Science Foundation of Yunnan Province (Nos. 2013HB097 and 2013FB083), and the Youth Innovation Promotion Association, CAS.

References

Ablimit, I., Xu, X.-j., & Li, X.-D. 2014, ApJ, 780, 80
Arnett, W. D. 1969, Ap&SS, 5, 180
Arnett, W. D. 1982, ApJ, 253, 785
Baraffe, I., Heger, A., & Woosley, S. E. 2004, ApJ, 615, 378
Brooks, J., Bildsten, L., Schwab, J., & Paxton, B. 2016, ApJ, 821, 28

Chen, W.-C., & Li, X.-D. 2009, ApJ, 702, 686
Chen, X., Han, Z., & Meng, X. 2014, MNRAS, 438, 3358
Chen, H.-L., Woods, T. E., Yungelson, L. R., Gilfanov, M., & Han, Z. 2015, MNRAS, 453, 3024
Denissenkov, P. A. 2012, arXiv:1210.7770
Denissenkov, P. A., Herwig, F., Bildsten, L., & Paxton, B. 2013, ApJ, 762, 8
Fang, J., & Zhang, L. 2012, MNRAS, 424, 2811
Gasques, L. R., Afanasjev, A. V., Aguilera, E. F., et al. 2005, Phys. Rev. C, 72, 025806
Greggio, L., & Renzini, A. 1983, A&A, 118, 217
Hachisu, I., Kato, M., & Nomoto, K. 1996, ApJ, 470, L97
Hachisu, I., Kato, M., Nomoto, K., & Umeda, H. 1999, ApJ, 519, 314
Hamuy, M., Phillips, M. M., Suntzeff, N. B., et al. 2003, Nature, 424, 651
Han, Z. 2008, ApJ, 677, L109
Han, Z., & Podsiadlowski, P. 2004, MNRAS, 350, 1301
Hayden, B. T., Garnavich, P. M., Kasen, D., et al. 2010, ApJ, 722, 1691
Hillman, Y., Prialnik, D., Kovetz, A., & Shara, M. M. 2016, ApJ, 819, 168 (arXiv:1508.03141)
Howell, D. A. 2011, Nature Communications, 2, 350
Hoyle, F., & Fowler, W. A. 1960, ApJ, 132, 565
Iben, Jr., I., & Tutukov, A. V. 1984, ApJS, 54, 335
Iglesias, C. A., & Rogers, F. J. 1996, ApJ, 464, 943
Israel, G. L., Stella, L., Angelini, L., et al. 1997, ApJ, 474, L53
Kasen, D. 2010, ApJ, 708, 1025
Kato, M., & Hachisu, I. 2004, ApJ, 613, L129
Khokhlov, A. M. 1991, A&A, 245, 114
Langer, N., Deutschmann, A., Wellstein, S., & Höflich, P. 2000, A&A, 362, 1046
Lesaffre, P., Han, Z., Tout, C. A., Podsiadlowski, P., & Martin, R. G. 2006, MNRAS, 368, 187
Li, X.-D., & van den Heuvel, E. P. J. 1997, A&A, 322, L9
Livne, E. 1990, ApJ, 354, L53
Ma, X., Chen, X., Chen, H.-l., Denissenkov, P. A., & Han, Z. 2013, ApJ, 778, L32
Maoz, D., Mannucci, F., & Nelemans, G. 2014, ARA&A, 52, 107
Matteucci, F., & Greggio, L. 1986, A&A, 154, 279
Neill, J. D., Sullivan, M., Howell, D. A., et al. 2009, ApJ, 707, 1449
Nomoto, K., Sugimoto, D., & Neo, S. 1976, Ap&SS, 39, L37
Nomoto, K. 1982a, ApJ, 257, 780
Nomoto, K. 1982b, ApJ, 253, 798
Nomoto, K., Thielemann, F.-K., & Yokoi, K. 1984, ApJ, 286, 644
Nomoto, K., Iwamoto, K., & Kishimoto, N. 1997, Science, 276, 1378
Parthasarathy, M., Branch, D., Jeffery, D. J., & Baron, E. 2007, New Astron. Rev., 51, 524
Patat, F., Chandra, P., Chevalier, R., et al. 2007a, Science, 317, 924
Patat, F., Benetti, S., Justham, S., et al. 2007b, A&A, 474, 931
Paxton, B., Bildsten, L., Dotter, A., et al. 2011, ApJS, 192, 3
Paxton, B., Cantiello, M., Arras, P., et al. 2013, ApJS, 208, 4
Paxton, B., Marchant, P., Schwab, J., et al. 2015, ApJS, 220, 15
Perlmutter, S., Aldering, G., Goldhaber, G., et al. 1999, ApJ, 517, 565
Piersanti, L., Tornambé, A., & Yungelson, L. R. 2014, MNRAS, 445, 3239
Podsiadlowski, P., Mazzali, P., Lesaffre, P., Han, Z., & Förster, F. 2008, New Astron. Rev., 52, 381
Riess, A. G., Filippenko, A. V., Challis, P., et al. 1998, AJ, 116, 1009
Ruiz-Lapuente, P., Comeron, F., Méndez, J., et al. 2004, Nature, 431, 1069
Taam, R. E. 1980, ApJ, 237, 142
Taubenberger, S., Benetti, S., Childress, M., et al. 2011, MNRAS, 412, 2735
Wang, B., Meng, X., Chen, X., & Han, Z. 2009a, MNRAS, 395, 847
Wang, X., Filippenko, A. V., Ganeshalingam, M., et al. 2009b, ApJ, 699, L139
Wang, B., & Han, Z. 2010a, MNRAS, 404, L84
Wang, B., & Han, Z.-W. 2010b, RAA (Research in Astronomy and Astrophysics), 10, 681
Wang, B., Li, X.-D., & Han, Z.-W. 2010, MNRAS, 401, 2729
Wang, B., & Han, Z. 2012, New Astron. Rev., 56, 122
Wang, B., Justham, S., Liu, Z.-W., et al. 2014, MNRAS, 445, 2340
Wang, B., Li, Y., Ma, X., et al. 2015, A&A, 584, A37
Webbink, R. F. 1984, ApJ, 277, 355
Whelan, J., & Iben, Jr., I. 1973, ApJ, 186, 1007
Woosley, S. E., & Weaver, T. A. 1986, ARA&A, 24, 205
Woosley, S. E., Wunsch, S., & Kuhlen, M. 2004, ApJ, 607, 921
Woudt, P. A., Steeghs, D., Karovska, M., et al. 2009, ApJ, 706, 738
Yang, C., Zhang, L., & Wang, J. 2015, MNRAS, 448, 3423
Yoon, S.-C., Langer, N., & Scheithauer, S. 2004, A&A, 425, 217
Yoon, S.-C., & Langer, N. 2005, A&A, 435, 967